

# Dielectric Function of Undoped and Doped Poly[2-methoxy-5-(3',7'-dimethyloctyloxy)-1,4-phenylene-vinylene] by Ellipsometry in a Wide Spectral Range

Jacek Gasiorowski,<sup>\*,†</sup> Kurt Hingerl,<sup>‡</sup> Reghu Menon,<sup>§</sup> Thomas Plach,<sup>‡</sup> Helmut Neugebauer,<sup>†</sup> Karin Wiesauer,<sup>||</sup> Cigdem Yumusak,<sup>⊥</sup> and Niyazi S. Sariciftci<sup>†</sup>

<sup>†</sup>Linz Institute for Organic Solar Cells (LIOS), Physical Chemistry, and <sup>‡</sup>Center for Surface and Nanoanalytics, Johannes Kepler University of Linz, Altenberger Strasse 69, 4040 Linz, Austria

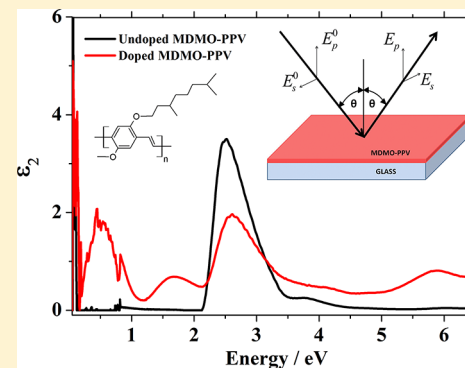
<sup>§</sup>Department of Physics, Indian Institute of Science, Bangalore 560012, India

<sup>||</sup>RECENTD Research Center for Non-destructive Testing GmbH, Altenberger Strasse 69, 4040 Linz, Austria

<sup>⊥</sup>Department of Physics, Faculty of Arts and Sciences, Yildiz Technical University, Davutpasa Campus, Esenler, 34210 Istanbul, Turkey

## Supporting Information

**ABSTRACT:** Ellipsometric measurements in a wide spectral range (from 0.05 to 6.5 eV) have been carried out on the organic semiconducting polymer, poly[2-methoxy-5-(3',7'-dimethyloctyloxy)-1,4-phenylene-vinylene] (MDMO-PPV), in both undoped and doped states. The real and imaginary parts of the dielectric function and the refractive index are determined accurately, provided that the layer thickness is measured independently. After doping, the optical properties show the presence of new peaks, which could be well-resolved by spectroscopic ellipsometry. Also for the doped material, the complex refractive index, with respect to the dielectric function, has been determined. The broadening of the optical transitions is due to the delocalization of polarons at higher doping level. The detailed information about the dielectric function as well as refractive index function obtained by spectroscopic ellipsometry allows not only qualitative but also quantitative description of the optical properties of the undoped/doped polymer. For the direct characterization of the optical properties of MDMO-PPV, ellipsometry turns out to be advantageous compared to conventional reflection and transmission measurements.



## INTRODUCTION

Organic semiconductors attract much attention due to their unique combination of interesting physical and chemical properties with easiness for their modifications, not only by chemical structure changes but also by oxidation or reduction procedures, usually called “doping”. The wide spectral characterization of organic semiconducting polymers is important from both fundamental and application points of view. In order to understand the optical properties due to doping, the variation of the complex dielectric function or, equivalently, the variation of the refractive index as a function of doping has to be measured. The imaginary part of the dielectric function is the characteristic response for allowed absorption processes, i.e., allowed optical transitions from initial states to excited states. For comparison of different materials this determination of optical constants is also important for applications such as organic light emitting diodes (OLEDs) as well as organic photovoltaics (OPV), since the optoelectronic properties of semiconducting polymers can be easily tuned by chemical substitutions for several applications. Also from fundamental aspects it is of considerable importance to

understand how the optical properties in these systems can be modified since the extent of  $\pi$ -conjugation and the stiffness of the backbone of the chains are highly susceptible to changes in the side groups. These features become even more significant by doping induced variations in the optical spectra, because the electrical (DC) conductivity of these systems can be altered by several orders of magnitude by chemical doping.

Usually the spectroscopic studies on these materials is performed either in the UV–vis<sup>1–3</sup> or in the IR region<sup>4–6</sup> employing transmission/reflection measurements giving transmittance and reflectance ( $T$ ,  $R$ ), which are both rather insensitive to the accurate determination of optical properties of thin layers. The measured quantities ( $T$ ,  $R$ ) are usually dominated by the reflection of the substrate. Hence a precise measurement of the optical parameters at various energy scales is very difficult. Also for the determination of spectral changes, e.g., when comparing spectra of doped samples to undoped

Received: June 23, 2013

Revised: September 3, 2013

Published: September 18, 2013

ones, the strong transmission/reflection of the substrate can be detrimental. In most of the current literature the relative variation of transmittance/reflectance is displayed, showing the change of the significant features after doping; however, the complex dielectric function  $\varepsilon_1(\omega) + i\varepsilon_2(\omega)$  or, equivalently, the complex refractive index  $n(\omega) + ik(\omega)$  is not determined.<sup>7–10</sup> The dielectric function represents a direct causal response function, which is not the case for a transmission/reflection measurement. In order to determine “absolute” (intrinsic, independent from measurement and geometry influences) material properties, these measurements have to be interpreted in terms of material response functions. The dielectric function gives the linear optical response. For pure substrates the dielectric function can be determined directly by spectroscopic ellipsometry. For thin unknown layers the dielectric function is more easily obtainable by modeling variable-angle spectroscopic ellipsometry data than normal incidence reflection and transmission data. Considerable work on the understanding and control of the optical properties of semiconducting polymers has been done in the past;<sup>11–15</sup> however, a crucial wide spectral range characterization in semiconducting polymers is often missing. Usually UV–vis  $R, T$  measurements detect relative changes in the absorption spectrum upon doping, where the main absorption peak of the undoped material decreases, and new peaks related to electronic changes in the semiconducting polymer appear. From Fourier transform infrared (FTIR) measurements only relative changes in  $R$  and  $T$ , due to the alterations in the vibrational structure as well as from formation of polaronic states, are usually obtained. Furthermore, if the spectra in these regions are taken separately, the response may appear at different scales, and a mismatch in the overall characterization of the optical properties in the broad spectral range can occur. Additionally, intensity measurements ( $R, T$ ) require background measurements or a light path and detector system calibration, and the experimental results sometimes show a nonlinear dependence on the intensity of the light beam.

In this study spectroscopic ellipsometry (SE), which allows direct optical characterization in a wide spectral range, was employed. With ellipsometry, the polarization state of the reflected/transmitted light is determined. A measurement of the absolute reflectivity is not required, just the complex ratio between the p- and s-polarized components; it is therefore rather insensitive to absolute intensities. Physical significance for SE measurement is obtained by interpreting the measured data with an optical model. Because SE measures directly two parameters ( $\psi$  and  $\Delta$ ) under different angles of incidence, the interpretation of the measured spectra in term of causal response functions, especially for thin overlayers, is much more reliable and more unique compared with  $R, T$  measurements, provided that the sample thickness is known. All measured data and transmission/reflection measurements, as well as ellipsometry measurements contain geometric parameters of the sample, such as, e.g., sample thickness.

For the determination of the absorption coefficient  $\alpha$  from  $R, T$  measurements usually Beer's law  $I(r_2) = I(r_1) \exp(-\alpha r_2 - r_1)$  is used, where  $\alpha$  is given by  $\alpha = 4\pi\kappa/\lambda_0$ , or equivalently by

$$\alpha = \frac{\varepsilon_2\omega}{cn} \quad (1)$$

where  $I(r_2)$  denotes the intensity at point  $r_2$  (it describes the light absorbed by passing from point  $r_1$  to point  $r_2$ ),  $\lambda_0$  is the wavelength of light in vacuum,  $\omega$  is the frequency, and  $c$  is the

speed of light in vacuum. However, this formula is only valid for thick films, where the coherent superposition of the fields between top side and bottom side reflection is negligible. Only then interference effects do not influence the measured spectra and a single absorption measurement can be used for the correct determination of  $\alpha$ . For thin films, the Fresnel reflectances as well as the phase acquired by multiply passing the layer have to be taken into account, demanding the use of equations involving the acquired phase (eqs 4.37–4.40 in ref 16), which refer to the optical path length (phase of the field), the (possibly complex) refractive index of the ambient and the substrate and the (complex) refractive index of the thin overlayer film.

In this work we present a comprehensive study of the optical properties of pristine and iodine doped MDMO-PPV by using spectroscopic ellipsometry. The obtained values for the real and imaginary part of the dielectric function ( $\varepsilon_1, \varepsilon_2$ ), or equivalently, for the real and imaginary part of refractive index ( $n, \kappa$ ) are given as a function of energy (or frequency)

$$\varepsilon(\omega) = \varepsilon_1(\omega) + i\varepsilon_2(\omega) = \tilde{n}(\omega)^2 = (n(\omega) + ik(\omega))^2 \quad (2)$$

The study was performed for a wide range of the energies between 0.05 (far-infrared) and 6.5 eV (far UV) of the undoped and doped polymer to determine precisely the differences in their optical properties. As a prerequisite for determining the correct refractive index of unknown samples, the thickness of the layer was determined independently for evaluating the dielectric function. As a material example we chose poly[2-methoxy-5-(3',7'-dimethyloctyloxy)-1,4-phenylene-vinylene] (MDMO-PPV), a semiconducting polymer well-known for preparation of organic solar cells and OLEDs.<sup>17</sup> The optical constants in the visible part of the spectrum, which were already calculated from the reflection/transmission measurement in the visible range by Hoppe et al.,<sup>18</sup> were taken for comparison. The ellipsometric results in the IR are additionally compared to FTIR data measured in the attenuated total reflection (ATR) mode.

## EXPERIMENTAL SECTION

In the study we used MDMO-PPV bought from Covion Co. The structure of the polymer is presented in Figure 1. The

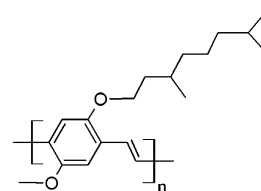


Figure 1. Chemical structure of MDMO-PPV.

polymer was used as received and dissolved in pyridine (99+%, Alfa Aesar) with concentration of 10 g L<sup>-1</sup>. For FTIR studies, ZnSe crystals were used as ATR elements. The crystals were precleaned by polishing with diamond paste (1 and 0.25  $\mu\text{m}$ ) and rinsing in a reflux system with acetone prior to measurement. A solution of the polymer was then spin-cast directly onto the ATR crystals, where, after drying, a film was formed. Infrared spectra were recorded with a FTIR spectrophotometer (Bruker IFS66S) with resolution of 4 cm<sup>-1</sup> at room temperature in ATR mode. In the setup a

mercury–cadmium telluride (MCT) detector cooled with liquid nitrogen prior to the measurements was used. During doping, ATR-FTIR spectra were recorded consecutively. By defining the first spectrum of the undoped material as a reference spectrum ( $T_{ref}$ ), and relating the subsequent spectra during doping ( $T_s$ ) to this reference spectrum, specific spectral changes during chemical oxidation were obtained. The difference spectra are calculated as  $\Delta\alpha d \propto -\log(T_s/T_{ref})$ .

For ellipsometric studies the solution was spin-coated onto  $15 \times 15 \text{ mm}^2$  glass slides, which were pre-cleaned by wiping with toluene and consecutive sonication in acetone (99.8%, NORMAPUR), 2-propanol (99.9%, NORMAPUR), and deionized water, and then dried by purging with air. By optimization it was found that the use of sonication in acetone, 2-propanol, and water decreases the hydrophilic behavior sufficiently to obtain smooth, thin layers of MDMO-PPV with high reproducibility of the thickness. The near-IR–vis–UV ellipsometric characterization was done using a Woollam M-2000 rotating compensator ellipsometer, which spans an energy range from 0.73 to 6.5 eV. The ellipsometric mid-IR and far-IR characterization was done using a Woollam IR VASE with  $32 \text{ cm}^{-1}$  resolution. This low resolution is due to the technical property of the ellipsometer, where the long acquisition time for rotating polarizers or compensators, as compared to the dedoping time of the polymer demands lower measurement resolution. The ellipsometric measurements were performed at three different angles of incidence ( $60$ ,  $65$ , and  $70^\circ$ ). All ellipsometry data were analyzed with WVASE software. The film thickness was determined using a Dektak XT Stylus profilometer. The samples were doped by exposure to iodine vapor for a duration of about 60 s.

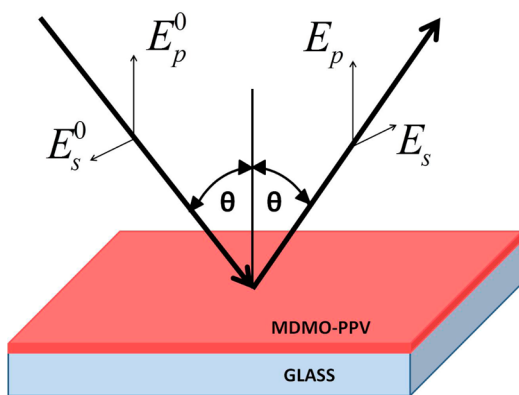


Figure 2. The basis of spectroscopic ellipsometry.

The scheme of spectroscopic ellipsometry is presented in Figure 2. With use of near-IR–vis–UV and IR SE setups, the complex reflectance ratio is determined by

$$\rho = \frac{r_p}{r_s} = \tan \psi e^{i\Delta} \quad (3)$$

where  $\rho$  is the ratio of the complex Fresnel reflection coefficients,  $r_p$  and  $r_s$  for p- and s- polarized light, respectively. The value  $\psi$  represents the absolute value of the ratio, and  $\Delta$  describes the phase difference between p- and s- polarized light.

## RESULTS AND DISCUSSION

In Figure 3a the measured ellipsometric angles  $\psi$  and  $\Delta$  of undoped and doped MDMO-PPV are presented for the UV–

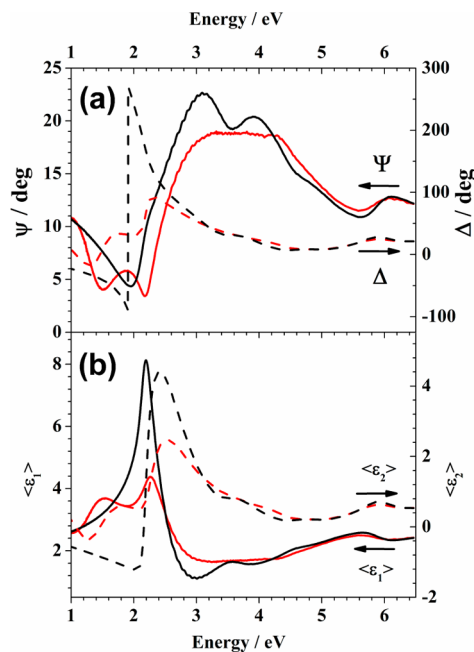


Figure 3. Results of the measurement using spectroscopic ellipsometry for undoped (black)/doped (red) MDMO-PPV. The measured complex ( $\psi$ ,  $\Delta$ ) quantity is plotted in (a), and the resolved complex pseudodielectric function MDMO-PPV is plotted in (b).

vis–near-IR region. As can be noticed, both ellipsometric angles are very sensitive to doping. In the graph the solid black and red lines represent the results of  $\psi$  obtained for the pristine/doped MDMO-PPV, respectively. The dotted black and dotted red lines plot the behavior of  $\Delta$  for the undoped/doped polymer. Changes in all spectral regions are observed, the strongest appearing in the vicinity of the expected resonances. The noticeable jump in  $\Delta$  for the undoped material (dotted black) is a simple “continuation”, because angles are measured in  $360^\circ$  intervals.

The measured complex quantity  $\rho = \tan \psi e^{i\Delta}$  can be converted to a complex pseudodielectric function  $\langle \epsilon(\omega) \rangle$  assuming that the multilayer can be described by a single and uniform dielectric layer, using<sup>19</sup>

$$\langle \epsilon_s \rangle = \epsilon_a \left( \sin^2(\theta) + \sin^2(\theta) \tan^2(\theta) \frac{(1 - \rho)^2}{(1 + \rho)^2} \right) \quad (4)$$

where  $\theta$  is the angle of incidence and  $\epsilon_a$  the dielectric function of the ambient, for air taken to be 1. If the sample under study is just a single homogeneous material, then the pseudodielectric function is the same as the dielectric function, representing the correct material response. If the sample is not a single homogeneous material, e.g., a thin layer on a substrate, eq 4 can be applied as well, assuming a single homogeneous substrate, but then the result is termed “pseudodielectric function” and indicated by  $\langle \epsilon \rangle$ . This pseudodielectric function is not an “absolute” physical quantity, because it also consists of geometrical and substrate properties and shows, e.g., interference oscillations. This pseudodielectric functions are shown in Figure 3b. Here the solid black and red lines describe

the behavior of the real part  $\langle \epsilon_1(\omega) \rangle$  for the undoped/doped material, respectively. The imaginary part  $\langle \epsilon_2(\omega) \rangle$  of the pseudodielectric function for the undoped/doped state of the polymer is displayed by the dotted black and dotted red lines, respectively. As mentioned, the pseudodielectric function, similar to  $R$ ,  $T$ , does not have a direct physical significance. This is best shown by pointing to the negative values of the imaginary part of the pseudodielectric function below 2 eV. It cannot be physically correct, since materials can only have positive (i.e., absorbing) imaginary parts of the material specific and system independent dielectric function. Here the negative value of  $\langle \epsilon_2(\omega) \rangle$  occurs due to interference. In order to determine the real dielectric function of the MDMO-PPV, first the dielectric function of the substrate (a thick glass slide with negligible roughness  $< 1$  nm) was determined. Using this, an optical model for the multilayer with the known thicknesses for air/MDMO-PPV/glass or, after doping, air/(MDMO-PPV) $^+I_3^-$ /glass, is set up. The dielectric function for the MDMO-PPV film is obtained by fitting the measured ellipsometric response,  $\psi$  and  $\Delta$ , using a complex model dispersion relation. At first fitting was performed for the angle of incidence  $65^\circ$ . For improving the sensitivity and accuracy the fitting was cross-checked afterward at other angles ( $60$  and  $70^\circ$ ). The MDMO-PPV thickness was determined by measuring the layer thickness at four positions with a stylus DEKTAK system before and after doping. The data were fitted using WVASE software with the known layer thickness, with the assumption of a negligible roughness, i.e., small compared to the wavelength, using a generic oscillator. As a result, a preliminary model for the real ( $\epsilon_1$ ) and imaginary ( $\epsilon_2$ ) part of the dielectric function was obtained. Then, the fitting was refined by either adding more oscillators, or a point to point fit, and checking the Kramers–Kronig consistency.

The values of the imaginary part of the dielectric function  $\epsilon_2$  as a function of wavelength are presented in Figure 4a. For pristine MDMO-PPV (plotted black), the single absorption peak with maximum at 2.5 eV is directly related to the optical band gap ( $\pi$ – $\pi^*$  transition) at 2.14 eV. After doping, the appearance of broad peaks at  $\sim 0.5$ , at  $\sim 1.7$ , and at  $\sim 5.9$  eV (plotted in red) is observed. The first two of these new peaks are related to transitions involving states within the gap, while the high-energy peak (at 5.9 eV) can be assigned to a new transition involving a higher state. After doping the value of the imaginary part of the dielectric function at 2.5 eV decreases by about half. The decrease of the main peak, together with the stronger appearance of the new peaks, is expected by considering the sum rule<sup>20</sup> for the dielectric function.

In agreement with the Kramers–Kronig relations,<sup>19</sup> similar enhancements can be observed for  $\epsilon_1$  plotted as a function of energy (Figure 4b). However, the Kramers–Kronig relations are integral relations covering all frequencies, and only for sharp (e.g., Lorentzian) transitions a direct correspondence within a finite energy interval is expected. For the pristine MDMO-PPV (plotted black) the presence of one main peak within the spectrum indicates that a single oscillator plays a dominant role. At higher energies, above the resonance frequency,  $\epsilon_1$  approaches 1.

After doping with iodine (Figure 4b, red) a decrease of the main oscillator strength occurs, with the appearance of two new oscillators with absorption maxima at 1.55 and 0.5 eV. Both can be attributed to the well-known formation of new levels in the band gap, related to polaronic transitions. Additionally a small shift of the main peak can be noticed with the new maximum at

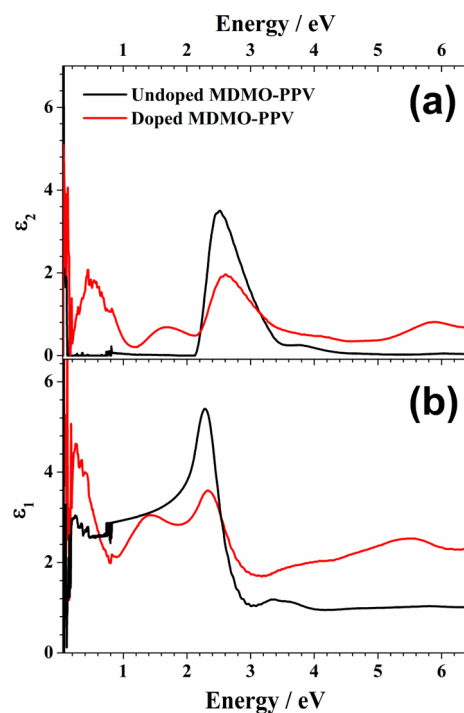


**Figure 4.** Imaginary (a) and real (b) parts of the dielectric function of undoped (plotted in black) and iodine doped (plotted in red) MDMO-PPV.

2.33 eV. In addition, the value of the real part of the dielectric function is doubled at low energies ( $< 0.7$  eV) compared to the undoped material.

For the infrared part of the spectrum, usually after doping, a broad transition in the IR, associated with polaron formation, and new dipole allowed infrared active vibrations (IRAVs) at lower energies appear. The IRAV bands can be described in different models, e.g., as a coupling between the electronic oscillations and the amplitude oscillation of the single/double bond alternation, introduced in the amplitude mode (AM) formalism by Horowitz et al.<sup>21,22</sup> Zerbi et al. have pointed out the correlation between the IRAV band and totally symmetric Raman modes in the effective conjugation coordinate (ECC) theory.<sup>23,24</sup> The connection between the doping induced electronic states and spectroscopically detected IRAV bands was formulated by Ehrenfreund and Vardeny.<sup>25</sup> The Girlando–Painelli–Soos (GPS) model describes the electron–phonon coupling.<sup>26,27</sup> However, all of these models describe the change in the absorption related to eq 1 and therefore require one to measure the real and imaginary parts of the dielectric function.

In Figure 5 the FTIR-ATR measurements (displayed as  $-\log(T_{\text{ATR}})$ ) are compared with the ellipsometric data. The FTIR-ATR differential spectrum of chemically doped MDMO-PPV is presented in Figure 5a (red curve). After exposure to iodine vapors the growth of a broad polaronic peak with a maximum at 0.48 eV is observed. Additional appearance of new infrared active vibrations with maxima at 0.187 and 0.14 eV can be noticed, in accordance with the theoretical models.<sup>21–27</sup>

Although FTIR measurements yield information about changes occurring in the vibrational structure of the polymer, it is very difficult to obtain the results in terms of the complex dielectric function or the refractive index. Similar to the UV–vis measurements, these disadvantages can be avoided using IR ellipsometry. However, compared to the ATR-FTIR technique,

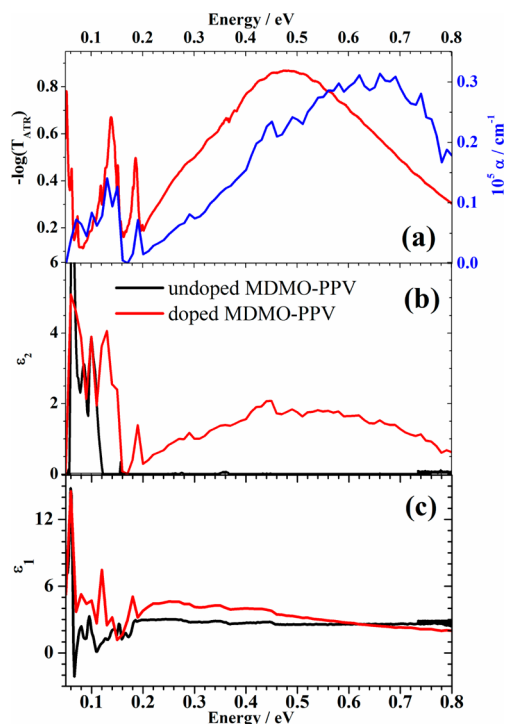


**Figure 5.** Doping induced changes measured by ATR-FTIR (red) and calculated absorption coefficient of the doped MDMO-PPV (blue) (a). Note that the doping induced changes can be easily measured with ATR, but for optical modeling the dielectric functions are necessary. Ellipsometric IR measurements: the imaginary (b) and real (c) parts of the dielectric function plotted as a function of energy for pristine (black) and doped (red) MDMO-PPV.

the peaks appear broader due to the lower spectral resolution ( $32\text{ cm}^{-1}$ ) in ellipsometry technique. The imaginary/real parts of the dielectric function obtained by IR ellipsometry are presented in Figure 5b/c. As can be noticed by comparison with the ATR-FTIR spectra shown in Figure 5a, a broad absorption peak with a maximum at  $\sim 0.5\text{ eV}$  due to the polaron formation can be found in the imaginary part, similar to the ATR measurements. The two peaks connected with new infrared active vibrational modes at 0.14 and 0.18 eV can be observed in both measurement techniques, and the imaginary dielectric function coincides with the peaks in ATR. Since the ATR-FTIR measurements detect the changes in the absorption coefficient, this coincidence can be expected from eq 1, since the energetic position is only slightly changing as long as the refractive index is rather constant and dispersionless. For the polaronic transition with maximum around 0.5 eV, the ATR absorption energy does not necessarily coincide with the absorption given by the absorption coefficient, because also changes in the real part of the dielectric function can become important, influencing the interaction of the evanescent wave with the absorbing material. This comparison is presented in Figure 5a, which compares the measured FTIR data (in red) with the calculated ellipsometric absorption data (in blue). The reason is that, especially for a spectrally broad absorption, the ATR measurement depends on the variation of the refractive index in the spectral range and, moreover, on the relation between the layer thickness, wavelength, and penetration depth.<sup>28</sup>

The real part of the dielectric function is presented in Figure 5c both for undoped (plotted in black) and doped (plotted in

red) MDMO-PPV. For the doped material the value of  $\epsilon_1$  in the energy range between 0.2 and 0.5 eV is a factor of 2 higher compared to the undoped sample. Strong changes of the real part of the dielectric function can be observed also in the fingerprint region below 0.2 eV due to strong doping induced dipole moment changes associated with the vibrations becoming IR active. Upon doping, the real part of dielectric function in IR varies significantly, suggesting that the absorption by the charged carriers is sensitive to the oscillators (IRAV, infrared active vibrations) with the respective reduction of the symmetry of the molecule.

The calculated absorption coefficient for the doped polymer in the UV-vis-near-IR is compared with the imaginary part of the dielectric function obtained by ellipsometry in Figure 6.

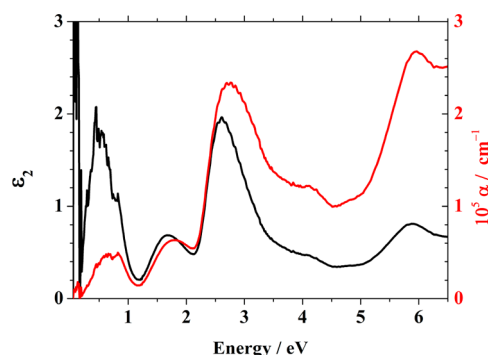


**Figure 6.** Broad spectral comparison between the imaginary part of the dielectric function (black) and the calculated absorption coefficient (red) for doped MDMO-PPV.

Differences are found, e.g., a stronger increase of  $\alpha$  with energy. In addition, the absorption coefficient has a different spectral shape than the imaginary part of the dielectric function in certain spectral ranges.

The real and imaginary parts of the refractive index  $\tilde{n} = n + ik$  are shown in Figure 7 for undoped and doped MDMO-PPV. The real and imaginary parts of the refractive index show the same behavior as the real and imaginary parts of the dielectric function. As in the case of  $\epsilon_1$ , the real part of the refractive index shows one peak for the pristine polymer. After doping, the value of the real part of the refractive index decreases and new peaks appear at lower energies. In addition, the refractive index at the oscillators decreases with doping, which is consistent with the electron sum rule.<sup>19,29</sup>

## CONCLUSION

This study shows that wide spectral characterization using ellipsometric spectroscopy is a powerful method to determine unambiguously the optical properties of semiconducting polymers in their pristine and doped form. The optical properties  $\epsilon_1(\omega) + i\epsilon_2(\omega)$ ,  $n(\omega) + ik(\omega)$  related to electronic transitions have been determined by spectroscopic ellipsometry in the range of 0.05–6.5 eV. This data set for the undoped and doped polymer can be found tabulated in the supplementary part and can also be requested from the authors. The benefit of ellipsometric measurements and the ellipsometric characterization in comparison to conventional R,T measurements has been discussed. The major additional information is related to the acquisition of two parameters ( $\psi$  and  $\Delta$ ), taken at different angles of incidence for corroborating measurements. By modeling these data for thin films the complex dielectric

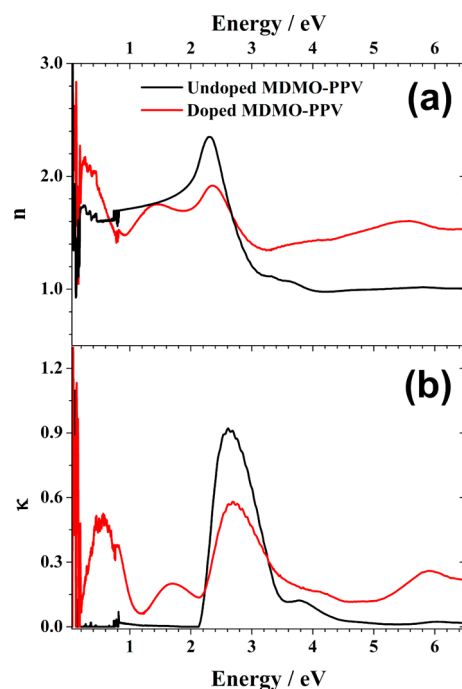


**Figure 7.** Calculated real (a) and imaginary (b) parts of the refractive index for undoped (black) and doped (red) MDMO-PPV plotted as a function of energy.

function can be determined directly, which is usually not the case for R, T measurements. As a major result of the MDMO-PPV doping study, the quantification of the optical properties of new electronic transitions at lower energy due to the “in-the-gap” transitions was possible with SE. It was found that the absorption peaks in the dielectric function are strongly dependent on doping. Especially for designing solar cells, the optical properties for each single constituent layer, given as  $\epsilon_1(\omega) + i\epsilon_2(\omega)$ , or as  $n(\omega) + i\kappa(\omega)$  have to be known for optimal light management.

## ■ ASSOCIATED CONTENT

### 📄 Supporting Information

Table showing the tabulated real and imaginary parts of the dielectric function of the pristine MDMO-PPV. This material is available free of charge via the Internet at <http://pubs.acs.org>.

## ■ AUTHOR INFORMATION

### Corresponding Author

\*E-mail: [jacek.gasiorowski@jku.at](mailto:jacek.gasiorowski@jku.at). Phone: +43 732 2468-8854. Fax: +43 732 2468-8770.

### Notes

The authors declare no competing financial interest.

## ■ ACKNOWLEDGMENTS

We gratefully acknowledge the financial support from Austrian Funds for Advancement of Science (FWF) within the Wittgenstein Prize scheme (Z 222-N19 Solare Energieumwandlung).

## ■ REFERENCES

(1) Xie, R. H.; Bryant, G. W.; Sun, G. Y.; Nicklaus, M. C.; Heringer, D.; Frauenheim, T.; Manaa, M. R.; Smith, V. H.; Araki, Y.; Ito, O. Excitations, optical absorption spectra, and optical excitonic gaps of

heterofullerenes. 1.  $C_{60}^{-}$ ,  $C_{59}N^{+}$ , and  $C_{48}N_{12}$ : Theory and experiment. *J. Chem. Phys.* **2004**, *120*, 5133–5147.

(2) Van Severen, I.; Breselge, M.; Fourier, S.; Adriaensens, P.; Manca, J.; Lutsen, L.; Cleij, T. J.; Vanderzande, D. 2,5-Substituted PPV-Derivatives with Different Polarities: The Effect of Side Chain Polarity on Solubility, Optical and Electronic Properties. *Macromol. Chem. Phys.* **2007**, *208*, 196–206.

(3) Rivaton, A.; Chambon, S.; Manceau, M.; Gardette, J.-L.; Firon, M.; Leaitre, N.; Guillerez, S.; Cros, S. Impact of light on organic solar cells: Evolution of the chemical structure, morphology, and photo-physical properties of the active layer. *Proc. SPIE* **2008**, *7002*, 70020L-1–70020L-12.

(4) Teketel, Y.; Neugebauer, H.; Farinola, G. M.; Winder, C.; Banudri, F.; Cardone, A.; Naso, F.; Sariciftci, N. S. Vibrational spectroscopic study of a push-pull substituted fluorinated poly(p-phenylenevinylene) copolymer. *Synth. Met.* **2005**, *152*, 149–152.

(5) Neugebauer, H.; Kvarnström, C.; Brabec, C.; Sariciftci, N. S.; Kiebooms, R.; Wudl, F.; Luzatti, S. Infrared spectroelectrochemical investigations on the doping of soluble poly(isothianaphthene methine) (PIM). *J. Chem. Phys.* **1999**, *110*, 12108–12115.

(6) Khatib, O.; Yuen, J. D.; Wilson, J.; Kumar, R.; Di Ventra, M.; Heeger, A. J.; Basov, D. N. Infrared spectroscopy of narrow gap donor–acceptor polymer-based ambipolar transistors. *Phys. Rev. B* **2012**, *86*, No. 195109.

(7) Otero, T. F.; Bengoechea, M. UV–Visible Spectroelectrochemistry of Conducting Polymers. Energy Linked to Conformational Change. *Langmuir* **1999**, *15*, 1323–1327.

(8) Teketel, Y.; Lattante, S.; Neugebauer, H.; Sariciftci, N. S.; Andersson, M. In situ FTIR spectroelectrochemical characterization of n- and p-dopable phenyl-substituted polythiophenes. *Phys. Chem. Chem. Phys.* **2009**, *11*, 6283–6288.

(9) Chazaro-Ruiz, L. F.; Kellenberger, A.; Dunsch, L. In situ ESR/UV–vis–NIR and ATR-FTIR spectroelectrochemical studies on the p-Doping of copolymers of 3-Methylthiophene and 3-Hexylthiophene. *J. Phys. Chem. B* **2009**, *113*, 2310–2316.

(10) Gasiorowski, J.; Glowacki, E. D.; Hajduk, B.; Siwy, M.; Chwastek-Ogierman, M.; Weszka, J. P.; Neugebauer, H.; Sariciftci, N. S. Doping-Induced Immobile Charge Carriers in Polyazomethine: A Spectroscopic Study. *J. Phys. Chem. C* **2013**, *117*, 2584–2589.

(11) Bredas, J. L.; Scott, J. C.; Yakushi, K.; Street, G. B. Polarons and bipolarons in polypyrrole: Evolution of the band structure and optical spectrum upon doping. *Phys. Rev. B* **1984**, *30*, 1023–1025.

(12) Patil, A. O.; Heeger, A. J.; Wudl, F. Optical Properties of Conducting Polymers. *Chem. Rev.* **1988**, *88*, 183–200.

(13) Moliton, A.; Hiorns, R. C. Review of electronic and optical properties of semiconducting  $\pi$ -conjugated polymers: Applications in optoelectronics. *Polym. Int.* **2004**, *53*, 1397–1412.

(14) Neugebauer, H. Infrared signatures of positive and negative charge carriers in conjugated polymers with low band gaps. *J. Electroanal. Chem.* **2004**, *563*, 153–159.

(15) Dunsch, L. Recent advances in in situ multi-spectroelectrochemistry. *J. Solid State Electrochem.* **2011**, *15*, 1631–1646.

(16) Azzam, R. M. A.; Bashara, N. M. *Ellipsometry and Polarized Light*; North Holland: Amsterdam, 1987.

(17) Shaheen, S. E.; Brabec, C. J.; Sariciftci, N. S.; Padinger, F.; Fromherz, T.; Hummelen, J. C. 2.5% efficient organic plastic solar cells. *Appl. Phys. Lett.* **2001**, *78*, 841–843.

(18) Hoppe, H.; Sariciftci, N. S.; Meissner, D. Optical constants of conjugated polymer/fullerene based bulk-heterojunction organic solar cells. *Mol. Cryst. Liq. Cryst.* **2002**, *385*, 113–119.

(19) Yu, P. Y.; Cardona, M. *Fundamentals of Semiconductors. Physics and Materials Properties*, 4th ed.; Springer: New York, 2010.

(20) Gasiorowski, J.; Menon, R.; Hingerl, K.; Dachev, M.; Sariciftci, N. S. Surface morphology, optical properties and conductivity changes of poly(3,4-ethylenedioxythiophene):poly(styrenesulfonate) by using additives. *Thin Solid Films* **2013**, *536*, 211–215.

(21) Horowitz, B. Infrared activity of Peierls systems and application to polyacetylene. *Solid State Commun.* **1982**, *41*, 729–734.

(22) Ehrenfreund, E.; Vardeny, Z.; Brafman, O.; Horovitz, B. Amplitude and phase modes in *trans*-polyacetylene: Resonant Raman scattering and induced infrared activity. *Phys. Rev. B* **1987**, *36*, 1535–1559.

(23) Zerbi, G.; Gussoni, M.; Castiglioni, C. Vibrational spectroscopy of policonjugated aromatic materials with electrical and non linear optical properties In *Conjugated polymers: Novel science and technology of conductive and non linear optically active materials*; Bredas, J. L.; Silbey, J., Eds.; Kluwer: New York, 1991; pp 435–507.

(24) Del Zoppo, M.; Castiglioni, C.; Zuliani, P.; Zerbi, G. In *Handbook of Conducting Polymers*, 2nd ed.; Skotheim, T. A., Elsenbaumer, R. L., Reynolds, J. R., Eds.; Marcel Dekker: New York, 1988; Chapter 28.

(25) Ehrenfreund, E.; Vardeny, Z. V. Phonon spectroscopy in  $\pi$ -conjugated polymers: The role of the excited electronic states. *Proc. SPIE* **1997**, *3145*, 324–332.

(26) Girlando, A.; Painelli, A.; Soos, Z. G. Electron-phonon coupling in conjugated polymers: Reference force field and transferable coupling constants for polyacetylene. *J. Chem. Phys.* **1993**, *98*, 7459–7465.

(27) Sariciftci, N. S.; Mehring, M.; Gaudl, K. U.; Bäuerle, P.; Neugebauer, H.; Neckel, A. Third Generation of Conducting Polymers: Spectroelectrochemical Investigations of Viologen Functionalized Poly(3-alkylthiophenes). *J. Chem. Phys.* **1992**, *96*, 7164–7170.

(28) Harrick, N. J. *Internal Reflection Spectroscopy*; Wiley: New York, 1967.

(29) Jones, W.; March, N. H. *Theoretical Solid State Physics: Non-Equilibrium and Disorder*, Vol. 2; Dover Publications: Mneola, NY, USA, 1985.